Numerical modelling and simulation
of liquid-impelled loop reactor

M.O. Daramola, A. Zampraka, E.F. Aransiola, G. A. Adeogun

Abstract. A liquid-impelled reactor (LLR) system was modelled using macro-and micro-balance technique. The relative goodness of using macro-balance was evaluated by comparing its solutions with the results obtained using micro-balance modell. The micro-balance modell formulated was used to investigate the dynamic behaviour of the system and to crosscheck the effectiveness of macro-balance modell. A numerical solution of the micro-balance modell was obtained, with which the system was simulated and the results were compared with the analytical solution of the macro-balance modell in order to compare their ability to effectively describe the system. The results showed a perfect correlation between the solutions obtained using analytical and numerical techniques. This is an indication that the system can be described or modelled using both microbalance and macro-balance. Also, the type of empirical correlation used to estimate the mass transfer coefficient influences the dynamic behaviour of the system.

1 Introduction

The liquid-impelled loop reactor (LLR), is a relatively novel type of bioreactor ([4]), analogous to the airlift loop reactor. In this reactor small droplets of an organic fluid are injected into a column of water (the riser). By the density difference between the organic and water phase, the droplet will rise. If a large amount of droplets are injected, they induce also flow in the water phase (it will be dragged along) via a loop connected from the top to the bottom of the column the water phase is circulated (see Figure 7). This kind of reactor can be used if one wants to extract some compound (reactant) from the aqueous phase, which has a low solubility in the aqueous phase but a high solubility in the organic phase. In this study we investigated the extraction of tetralin (an anti-biotic), a compound produced by microorganisms. The organisms expel the compound from their cells into the aqueous phase. At high concentrations tetralin is toxic for the organisms, and therefore would retard the growth of the

organisms (and thus its own production). This can be prevented if the organic solvent extracts tetralin. At the top of the column the organic solvent accumulates, and is led to an adsorption column for downstream processing. Another major advantage of the liquid loop reactor (over stirred reactors) is the avoidance of high-shear regions. ([1]). However, efficiency of this reactor depends on the size of the liquid droplets. The size of the liquid droplets is determined by the orifice diameter. At the same time optimal droplet size is needed for optimal tetralin extraction. Therefore, this study tries to find the optimal droplet size for the optimal tetralin extraction. Meanwhile, this paper presents the possibility of modelling the system with a single macro-balance using numerical modelling technology which offers an efficient and powerful tool for simulating processes in chemical, biochemical, bioprocessing or food industries ([6]).

2 Mathematical modell formulations

The mathematical modells used in this study comprise the hydrodynamic equations; mass microbalance and mass transfer equations. For modell simplicity, some assumptions were taken. A single droplet of tetralin is considered with the assumption that the concentration of tetralin in the aqueous phase is constant and uniform. It was assumed an isothermal LLR with the mass transfer dictated by Ficks law. Some parameters such as diffusion coefficients of the tetralin in water and solvent, water/solvent partition coefficient, density of the solvent and the height of the riser were assumed and taken from literature. These values are contained in Table 1.

2.1 *Hydrodynamics*

For the hydrodynamics, Bernoulli equation and Stokes law were employed. The average flow velocity u_{avg} is given by Bernoulli-equation as

$$(2.1) \qquad (1 - \varepsilon) * \Delta\rho * g = \frac{1}{2} * K_f * \rho_w * u_{avg}^2 \qquad \text{(Bernoullis equation)}$$

The driving force for the flow, which is the difference in hydrostatic pressure between riser and downcomer, for which the density difference ($\Delta\rho$) was defined as

$$(2.2) \qquad \Delta\rho = \rho_w - \rho_d$$

where ρ_w is the density of water and K_f, is the Fanning friction coefficient, assumed to be 5. The average velocity relates to the actual velocities of the phases as:

$$(2.3) \qquad u_{avg} = \varepsilon * \nu_c + (1 - \varepsilon) * \nu_d$$

The relation between dispersed phase velocity and average velocity was computed according to Zuber and Findlay ([7],[8]) as:

$$(2.4) \qquad \nu_d = u_{avg} + \nu_{\inf}$$

with ν_{inf} the terminal velocity of a isolated droplet followed the Stokes law and was given as:

(2.5)
$$\nu_{\text{inf}} = \Delta\rho * g * d_p^2 * \frac{1}{18 * \mu_w}$$

The volumetric flow rate of the dispersed phase is related to ν_d, as:

(2.6)
$$\phi_d = (1 - \varepsilon) * A * \nu_d$$

Equations (1) to (4) represent a system of non-linear equations, which was solved in Matlab ([2]) using a developed function fzero ([5]). A matlab function(LLR-hydro) was developed to compute the ε, volume fraction (hold up) of the continuous phase (porosity), ν_d, actual velocity of the droplets (dispersed phase) and ν_c, the actual velocity of the continuous phase with volumetric flow rate of the dispersed phase (ϕ_d), the height of the riser (H), the density of the organic (dispersed) phase (ρ_d), the cross sectional area of the riser (A), and the droplet diameter (d_p) specified (see Table 1).

2.2 *Mass balance and mass transfer equations*

The system was divided into two subsystems consisting the water phase containing water and tetralin and the organic phase containing tetralin and the solvent. Also in order to investigate the mass transport of tetralin into the droplet, the droplet was subdivided in spherical shells (control volumes) of length:

(2.7)
$$\Delta r = \frac{R}{N}$$

where N is the number of shells and R is the radius of the droplet. A schematic of the system is given in Figure 1 and Figure 2 shows the network representation of the system.

2.2.1 *mass microbalance*

The mass microbalance is

(2.8)
$$\frac{dM_n}{dt} = J_n - J_{n+1}$$

with J_n, the mass flux of tetralin from water to the solvent droplet;J_{n+1}, mass flux leaving shell n (entering $n+1$); J_{n+1}, mass flux leaving shell $n+1$ (entering n); M_n, mass of tetralin in the nth control volume.

2.2.2 *Constitutive equations*

The mass of tetralin in shell n is given as:

(2.9)
$$M_n = C_n * V_n$$

and the control volume is given as:

(2.10)
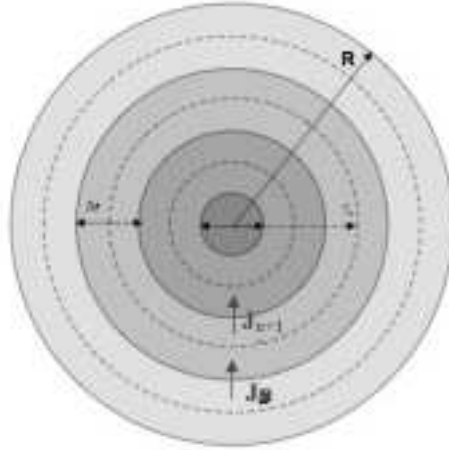$$\Delta V_n = \frac{4}{3} * \left[(r_n + 0.5 * \Delta r)^3 - (r_n - 0.5 * \Delta r)^3 \right]$$

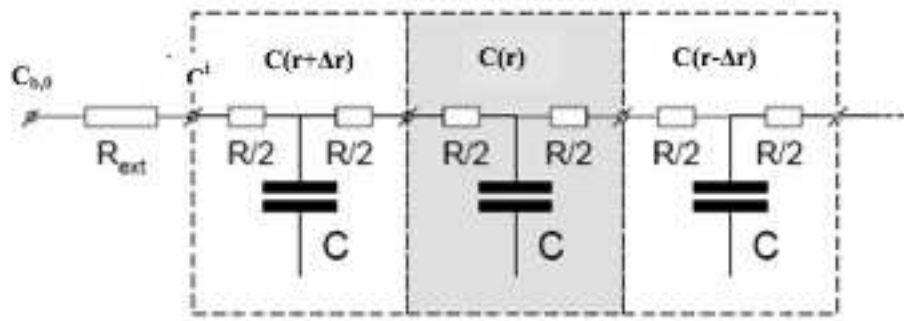Figure 1: Schematic of an organic solvent droplet divided in spherical shells

Figure 2: Network representation of the LLR system

if $\Delta r << R$,then;

(2.11)
$$V_n = 4 * \pi * r_n^2 * \Delta r$$

with V_n, the volume of tetralin in the nth control volume; r_n, the radius of the nth control volume and C_n, the concentration of tetralin in the nth control volume.

2.2.3   *Flux equations*

Due to the difference in solubility of tetralin in water and the organic solvent, there is a jump in concentration across the water/solvent interface. This situation is described

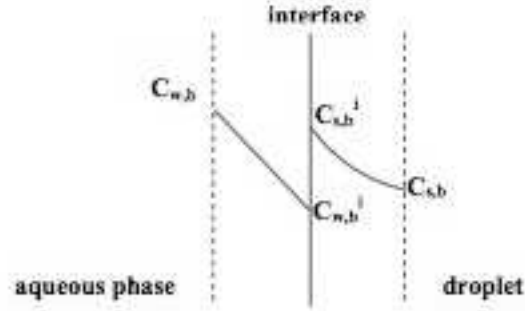in Figure 3 and with a simplified network diagram shown in Figure 4.

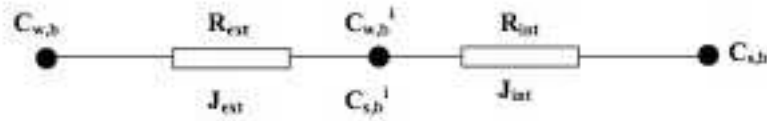Figure 3: Transport of tetralin across the interface

Figure 4: Simplified network dagram of Figure 3

With Ficks law assumed, the following equations were obtained:

$$(2.12) \qquad J_{\text{int}} = -\frac{C_{s,b} - C_{s,b}^i}{R_{\text{int}}}$$

$$(2.13) \qquad J_{\text{ext}} = -\frac{C_{w,b}^i - C_{w,b}}{R_{\text{ext}}}$$

where $J_{\text{ext}}, J_{\text{int}}, R_{\text{ext}}$ and R_{int}, are external flux, internal flux , internal resistance and external resistance respectively. With $J_{\text{int}} = J_{\text{ext}} = J_o$ and $C_{s,b}^i = k * C_{w,b}^i$, equation (2.12) and (2.13) become

$$(2.14) \qquad J_o = -\frac{C_{s,b} - k * C_{w,b}}{k * R_{\text{ext}} + R_{\text{int}}} = V_{tot}\frac{dC_{s,b}}{dt}$$

$$(2.15) \qquad \frac{dC_{s,b}}{dt} = \frac{C_{s,b} - k * C_{w,b}}{\tau}$$

Integrating equation (2.15) with concentration of tetralin from C_1 to C_{predav} gives

$$(2.16) \qquad C_{\mathrm{predav}} = k * C_{w,b} + (C_1 - K * C_{w,b}) * e^{\frac{-t}{\tau}}$$

where C_{predav}, the predicted average tetralin concentration in the droplet and C_1, the concentration in the first shell $= C_{w,o}$.
Equation (2.16), the analytical solution of the micro-balance equations, was used to compute the predicted average concentration in the droplet as a function of time and compare the results thereof with the solution obtained from the numerical integration.

2.2.4 *Flux equations in the droplet*

Assuming the Ficks law, the following equations were obtained for the mass transfer in the droplet.

$$(2.17) \qquad J_n = D_s * A_n * \frac{C_n - C_{n-1}}{\Delta r} = (C_n - C_{n-1}) * \frac{1}{R_n}$$

$$(2.18) \qquad J_{n+1} = D_s * A_n * \frac{C_{n+1} - C_n}{\Delta r} = \frac{C_{n+1} - C_n}{R_{n+1}}$$

$$(2.19) \qquad R_n = \frac{\Delta r}{(D_s * A_n)}$$

$$(2.20) \qquad R_{n+1} = \frac{\Delta r}{(D_s * A_{n+1})}$$

2.2.5 *Boundary Conditions*

For $n = 1$:

$$(2.21) \qquad J_1 = \frac{k * C_{w,b} - C_1}{R_{ov1}}$$

with

$$(2.22) \qquad R_{ov1} = (0.5 * R(1) + k * R_{\mathrm{ext}})$$

where R_{ov1}, is the combined resistance at $n = 1$ and $(n-1)^{th}$ shell. For $n = n + 1$, in the centre of the droplet:

$$(2.23) \qquad J = 0$$

2.2.6 *Mass transfer coefficient*

Mass transfer coefficient was obtained using two different empirical correlations to determine the Sherwood number with which the mass transfer coefficient as obtained.

This approach will assist to identify better empirical correlation for optimal design. The empirical correlations employed are contained in equations (2.24) and (2.25).

(2.24)
$$\mathrm{Sh}_1 = 2 + 0.95 * (Re * S_c)^{0.5}$$

(2.25)
$$\mathrm{Sh}_2 = 2 + 0.66 * (Re)^{0.5} * (S_c)^{0.33}$$

The Reynolds number,Re,and the Schmidt number,Sc, were obtained using equations (2.26) and (2.27), respectively. The mass transfer coefficient was caculated using equation (2.28).

(2.26)
$$Re = \frac{\nu_d - \nu_c * d_p}{\mu}$$

(2.27)
$$\mathrm{Sc} = \frac{\mu}{\rho * D_w}$$

(2.28)
$$\beta = \frac{\mathrm{Sh} * D_w}{d_p}$$

2.2.7   *Time constant analysis*

Substituting equations (2.9), (2.17) and (2.18) in equation (2.8) gives,

(2.29)
$$\frac{dC_n}{dt} = \frac{C_{n-1} - C_n}{V_n * R_n} - \frac{C_n - C_{n+1}}{V_n * R_{n+1}}$$

where

(2.30)
$$\tau_n = R_n * V_n$$

and

(2.31)
$$\tau_{n+1} = R_{n+1} * V_n$$

and

The time step for numerical integration was defined as:

(2.32)
$$\Delta t = \frac{\min(\tau_n)}{6} = \frac{\min(R_n * V_n)}{6}$$

Therefore, equations (2.30) and (2.31) were used in the numerical solutions of the LLR.

3   Solution of the modell equations

Main programs and subroutine were developed to solve the modell equations (19) and (28). The hydrodynamics was solved using a matlab program LLR-Hydro as a subroutine to the main program. From these solutions comparison was made.

4 Results

The results of the implementation of the matlab programs are shown in Figures 5 and 6.For $Sh_1 = 2 + 0.95 * (Re * Sc)^{0.5}$ and
$C_{\text{predav}} = \frac{M_{tot}}{V_{tot}}$,concentration profiles of tetralin in the organic solvent droplet is given in Figure 5.
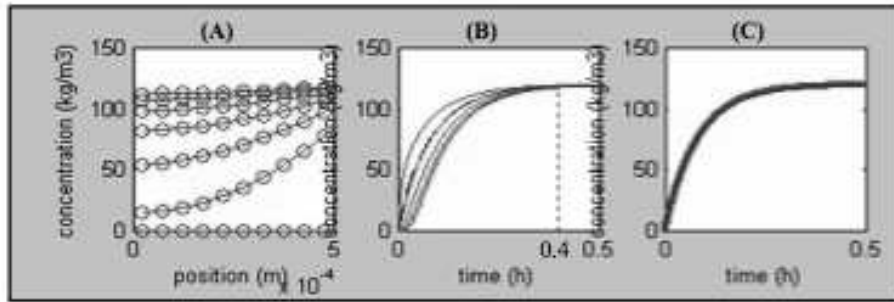

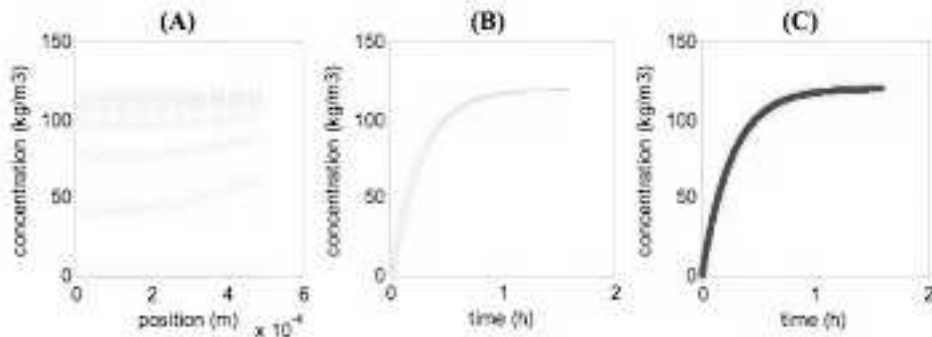Figure 5: Concentration profiles of tetralin in the organic solvent droplet using Sh1

Figure 6: Concntration profile of tetralin in the organic solvent using Sh2

For $Sh_2 = 2 + 0.66 * (Re)^{0.5} * (Sc)^{0.33}$ and
$C_{\text{predav}} = k * C_{w,b} + (C_1 - k * C_{w,b})e^{\frac{-t}{\tau}}$, Figure 6 shows the concentration profiles of tetralin in the organic solvent droplet.

Where (A), the concentration of tetralin in different positions in the droplet (centers of control volumes); (B) the concentration of tetralin as a function of time (the different lines represent different positions in the droplet (centers of control volumes); (C), the mean concentration of tetralin in the droplet. The blue line represents the

average concentration calculated from the numerical solution of the microbalances. The red line represents the average concentration predicted by the analytical solution.

5   Discussion of results

Figures 5 and 6 present the system under the use of the two different correlations to estimate the Sherwood number and two different expressions obtained from solving mass balance equations.

For $Sh_1 = 2 + 0.95 * (Re * Sc)^{0.5}$, the system shows a faster response (see Figure 5) leading to a $\tau_{RC1} \approx 300 sec$. For $Sh_2 = 2 + 0.66 * (Re)^{0.5} * (Sc)^{0.33}$, the system shows a slow response (see Figure 6) with a $\tau_{RC2} \approx 900 sec$. Hence, the steady state of the latter system is expected to be attained at $3 * \tau_{RC1}$.

Also,from Figures 5 (A) and 6 (A), it is observed that in the beginning of the process, a concentration gradient is formed along the diameter of the droplet. As the driving force for transfer (e.g. the concentration difference between the water phase and the droplet) reduces, the concentration gradient diminishes, until equilibrium is reached (steady state). At this point, the concentration along the droplet is the same everywhere and equal to 120 kg/m^3.

Figures 5 (B) and 6 (B) show that the tetralin concentration increases exponentially in time and steady state is reached when time $\approx$ 0.4 hours (for Sh_1) and 1 hour (for Sh_2), respectively. It is important to notice that the average concentration follows exponential increase to a limit.

Figures 5 (C) and 6 (C) show the average concentration in the droplet with two different modells, one based on microbalances and obtained from the numerical solution (see Figure 5C) and the second based on a single macrobalance obtained from the analytical solution of the microbalances (see Figure 6C).The two figures are very similar with the same dynamics except that one is faster than the other.

6   Conclusions

The two solutions obtained in this study are perfectly correlated and this is an indication that the system can be described with a single macrobalance derived from the analytical solution. Also the time to attain a steady state is influenced by the type of empirical correlation used to estimate the mass transfer coefficient.

References

[1] D.M.R. Mateus, M.M.R. Fonseca, S.S. Alves, *Hydrodynamics and mass transfer in Liquid-impelled loop reactor*, Ind. Eng. Chem. Res. 35 (1996), 4559-4565.

[2] MATLAB version 7.1.0.246 (Release 14), Math Works Inc, Prentice Hall, Englewood Cliffs, NJ 07632 ,2005.

[3] R.H. Perry, D.W. Green, *Perrys Chemical Engineers Handbook*, 8th ed., McGraw-Hill Book Company, New York, 2007.

[4] J. Tramper, I. Wolters, P. Verlaan.. *The liquid-impelled-loop reactor: a new type of density-difference-mixed bioreactor*, Studies in organic chemistry 29 (1987), 311-316.

[5] R.G.M van der Sman, *Lecture notes on advanced course in transfer processes in food and bioprocess engineering*, unpublished, Wageningen University and Research Centre, The Netherlands, 2005.

[6] L. Wang, D. Sun, *Recent developments in numerical modelling of heating and cooling processes in the food industry: a review*, Trends in Food Science and Technology 14 (2003), 779-809.

[7] N. Zuber, J.A. Findlay, *Average volumetric concentration in two-phase flow systems*, ASME J. Heat Transfer 87 (1965), 453.

[8] N. Zuber, J.A. Findlay, *General Electric Report* GEAP-4592, 1964.

Nomenclature

R_n	Resistance in n^{th} shell (s/m3)
R_{n+1}	Resistance in $(n+1)^{th}$ shell (s/m3)
d_p	Diameter of the droplet in m
D_w	Diffusivity of water in m2/s
C_n	Concentration of tetralin in nth shell
C_{n-1}	Concentration of titration in $n-1$ shell
V_n	n^{th} shell volume
D_s	Diffusivity of solvent in m2/s
$C_{w,b}$	Bulk concentration of tetralin in aqueous phase (mol/m3)
$C_{w,b}^i$	Interface concentration of tetralin in aqueous phase (mol/m3)
$C_{w,b}^i$	Interface concentration of tetralin in organic phase (mol/m3)
R_{ext}	External resistance (s/m3)
J_{int}	Internal flux
J_{ext}	External flux
C_{predav}	Predicted average concentration of tetralin (mol/m3)
J_n	Flux of tetralin into nth shell
J_{n+1}	Flux of tetralin into $(n+1)^{th}$ shell
Δr	Shell thickness
R	Radius of the control volume (m)
β	Mass transfer coefficient (m2/s)
μ	Dynamic viscosity of water (Pa.s)
ρ_s	Density of the solvent (kg/m3)
ρ_w	Density of water (kg/m3)

Table 1: Constant parameters used for simulation [3]

| S/N	parameters	values
1	Water diffusivity (m^2/s)	$7.2 * 10^{-10}$
2	Solvent diffusivity (m^2/s)	$14 * 10^{-10}$
3	Water/solvent partition coefficient $(k_{w/s})$	1/120
4	Height of riser (m)	0.5
5	Density of the solvent (kg/m^3)	970
6	Tetralin concentration in aqueous solution (mol/m3)	1.0
7	Density of water (kg/m^3)	1000
8	Dynamic viscosity of water (Pa.s),μ	10^{-3}
9	Diameter of a droplet (m)	0.05
10	Fanning factor, f	5
11	Gravitational constant (m/s^2), g	9.8
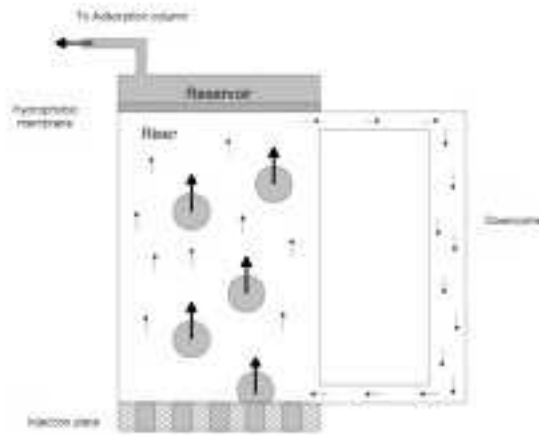
Figure 7: Schematic of liquid-impelled loop reactor (LLR)

Authors' addresses:

Michael O. Daramola (corresponding author)
Current address: Stellenbosch University, Private Bag X1,
Matieland 7602, Stellenbosch, South Africa.
Permanent address: Chemical Engineering, Obafemi Awolowo University,
Ile Ife, Nigeria.
E-mail: daramola@sun.ac.za

Apostolia Zampraka
Bioprocess Engineering, Wageningen University and Research Centre,
The Netherlands.
E-mail:bofakau@yahoo.com

Elizabeth .F. Aransiola
Chemical Engineering, Obafemi Awolowo University, Ile -Ife, Nigeria
E-mail: aransiola4@yahoo.com

Ganiyu. A. Adeogun
Present address: Integrated Urban Engineering, UNESCO-IHE, Delft,
The Netherlands.
Permanent address: Civil Engineering, University of Ibadan, Ibadan, Nigeria.
E-mail: adeog1@unesco-ihe.org